

# Electro-Optic, Multi-spectral, Detection of Scatterable Landmines

*John A. Coath and Mark A. Richardson  
Department of Aerospace, Power and Sensors  
Cranfield University, Royal Military College of Science  
Shrivenham, Swindon, Wilts, United Kingdom*

## Abstract

Representative scatterable anti-personnel landmines have been examined at electro-optical wavelengths from 200 nm to 14  $\mu\text{m}$ . Diffuse and specular reflections have been measured and these results are compared with potential backgrounds in which such anti-personnel mines could be sown. From this data regions of particular interest due to high contrast are extracted, and proposals are made for exploitation for a simple, low-cost mine detector. In regions where there is inherent high clutter polarization discrimination is proposed to augment the contrast. Experimental work to illustrate the practicability of these devices has been undertaken and is presented here.

## Introduction

The Ottawa Treaty of 1997<sup>1</sup> banning anti-personnel landmines has had little influence on the perceived threat that such devices pose as several major producers and suppliers have yet to sign and large areas of the globe are still heavily contaminated with mines laid in previous decades. Scatterable anti-personnel mines are readily dispersed by artillery, rockets, aircraft, and ground vehicles, for area denial, to restrict enemy movement and to impede clearance of conventional minefields. Anti-personnel mines are difficult to detect as they are laid at random, have minimal metallic content and are camouflaged to visual detection.<sup>2</sup> In most cases mine clearance requires some form of mine detection, either to map the extent of contamination or as an initial stage of the removal and destruction process. The aim of this work was twofold, firstly to find regions of the electromagnetic spectrum where scatterable anti-personnel landmines show high contrast against their backgrounds, and secondly to augment low contrast regions by reducing the clutter in natural backgrounds.

## Experimental

Four representative scatterable anti-personnel landmines, examples of which were readily available, were examined in this work, namely, P-4-B (Spain), PFM-1 (Russia),

Ranger (UK), and SB-33 (Italy). All except Ranger have been widely deployed in Africa, the Falkland Islands, and Afghanistan.

Over the ultra-violet, visible and near-infrared portions of the electromagnetic spectrum, contrast may be defined in terms of the reflectivities,  $R$ , of the target (mine) and background as:

$$\text{Contrast} = \frac{R_{\text{target}} - R_{\text{background}}}{R_{\text{target}} + R_{\text{background}}} \quad (1)$$

The generally accepted threshold of visibility for the human eye is a contrast between 2% and 5%.

In the far-infrared where scenes are typically emission dominated<sup>3</sup> the contrast can be given as:-

$$\text{Contrast} = \frac{\text{Power}_{\text{target}} - \text{Power}_{\text{background}}}{\text{Power}_{\text{target}} + \text{Power}_{\text{background}}} \quad (2)$$

Mines are generally well camouflaged to visual observation, making them difficult to detect even at short range. Their contrast at thermal infrared wavelengths is also low under most conditions, as their small mass limits their temperature differential to the background and their emissivities are broadly similar to soil and vegetation. This work concentrated on two areas, determining the potential contrast by reflection of scatterable anti-personnel landmines in the ultra-violet (UV) and near-infrared (NIR) spectral bands and augmenting the contrast in the far-infrared (FIR) spectral region by utilizing a polarization technique.

Measurements were made of diffuse reflectance at UV, visible and NIR wavelengths using a Perkin-Elmer Lambda 9 spectrophotometer. Measurements at UV and visible wavelengths were made using a 150 mm diameter integrating sphere, referenced to a high reflectance diffuse white standard (Labsphere, Inc. Spectralon). This integrating sphere did not operate at NIR wavelengths, so a specular reflectance jig was used with the same Spectralon block as standard and a reference beam attenuator to balance the intensity in the sample and reference beams of the spectrophotometer. This arrangement produced good

reflectance spectra, but can be subject to error if the specimen under measurement shows some gloss. In this case falsely high readings of reflectance will be obtained. The mines measured in this work did not show appreciable gloss to visual observation so the reflectivities are considered reliable, however, no great accuracy is claimed for these measurements, as the aim was to identify regions with significant reflectivity differences that would show high contrast, and not to measure reflectivity to high accuracy.

Reflectances taken from the mines were compared to those of grass and soil. The grass specimen was prepared by placing several layers of freshly cut grass leaves on to a matt black painted block to completely cover the block. The leaves were held in place by taping their ends to the block, leaving the centre section clear for measurement. A soil compact was made by pressing soil into a short length of tube placed on a flat glass plate. After compression, the glass was removed leaving a flat surface to the soil specimen held in the tube.

Measurements in the far-infrared were made using a Perkin-Elmer 983 spectrophotometer. The system was set up to measure specular reflectance at an angle of incidence of 30° (representative of a suspended or overflying mine detector). The mine was illuminated with linearly polarized radiation by placing an infrared polarizer in the source beam and reflected radiation was analysed by a second polarizer in the common beam of the instrument. 0° and 90° polarization states were measured.

## Results

### Ultra-violet and Visible Measurements

Reflectance spectra for the four mines, measured using the integrating sphere over the wavelength range 250 nm to 450 nm, are presented in Figure 1 together with the reflectances of grass and soil which are given for comparison. No correction has been made to the measured data for the reflectance of the white Spectralon reflectance standard.

Across the ultra-violet wavelength range, 250 nm to 400 nm, grass and soil show closely similar, low reflectances in the 2.5% to 3.5% range. All of the mines show higher reflectances in this spectral region.

P-4-B shows a fairly uniform 8% to 9% reflectance, and PFM-1 6% to 7% except close to 400 nm where reflectance increases sharply towards a peak of 13% at 410 nm at the violet end of the visible spectrum (Figure 1). The Ranger mine showed a largely featureless reflectance spectrum in this wavelength range with values in the 5% to 7% range whilst SB-33 showed a broad minimum in reflectance at about 330 nm at a little over 5%

### Contrast in the Ultra-Violet Waveband

All mines showed substantial positive contrast to grass and soil. Calculation of contrast at mid band for ultra-violet wavelengths gave values of at least 30%. P-4-B was

exceptionally high at 53% with the remaining mines showing 30% to 35% contrast.

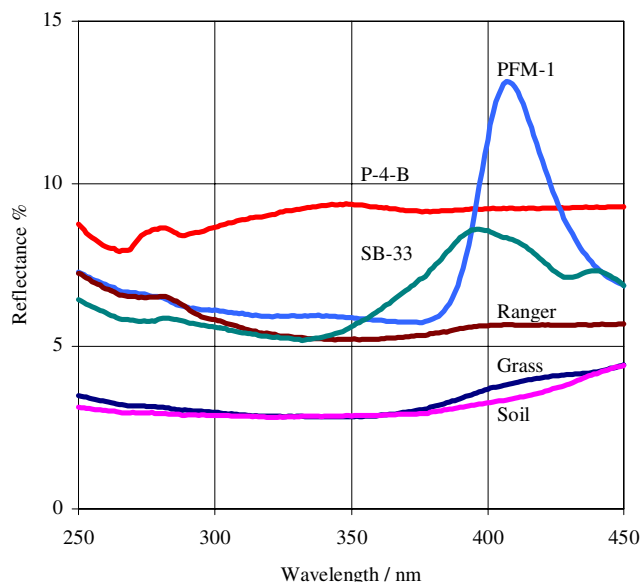


Figure 1. Ultra-violet Reflectance of Mines

### Contrast in the Visible Waveband

At visible wavelengths the situation is much more complicated owing to the reflectance changes across the band by the grass, the soil and the mines themselves. This would result in the mines giving positive contrast at some wavelengths and negative contrast at others. It is however well known that these mines can be very difficult to detect visually even at short ranges of ten metres or so.

### Near-Infrared Measurements

Data are presented from the red end of the visible spectrum across part of the near-infrared waveband (650 nm to 1200 nm) for the four mines, grass, and soil in Figure 2. These measurements were made using the specular reflectance jig referenced to a diffuse white standard.

In this waveband there are significant differences between the reflectances of grass and soil, most notably about 700 nm where the reflectance of grass changes from 5% to about 70% over a narrow wavelength interval. This so-called "chlorophyll edge" is a feature of all living vegetation. The high reflectance of grass is maintained to about 1200 nm and then decays at longer wavelengths. Soil showed moderate reflectance in the NIR waveband, generally between 15% and 28%.

The mines fall into two groups, those which mimic the increased reflectance of living vegetation at about 700 nm and then show reflectances between grass and soil (PFM-1 and Ranger) and those which do not and show fairly uniform low reflectance over the entire band (P-4-B and SB-33).

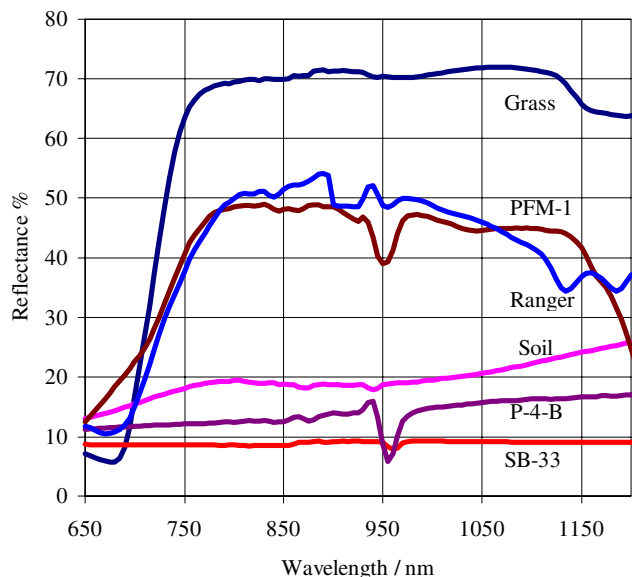


Figure 2. Near-infrared Reflectance of Mines

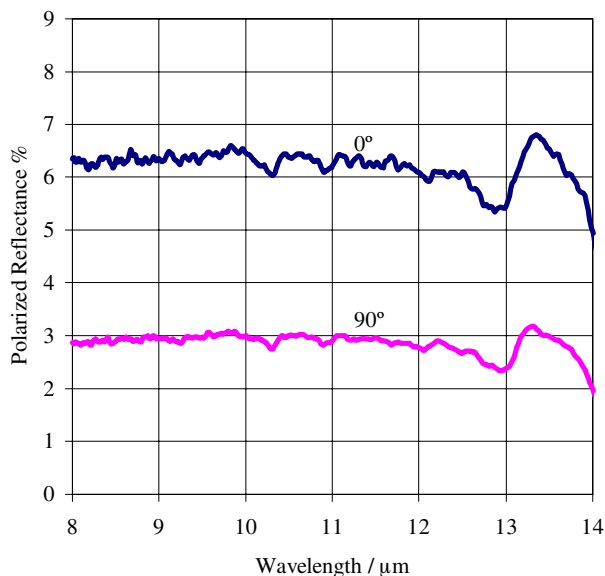


Figure 3. P-4-B Mine Polarized Reflectance

PFM-1 and Ranger (Figure 2) show a large increase in reflectance close to 700 nm reaching about 50% at 800 nm before values decrease at longer wavelengths. Several reflectance dips, presumably associated with absorption bands in the polymer cases, are evident in the spectra. The P-4-B and SB-33 mines show lower reflectance than soil over all of the waveband.

#### Contrast in the Near Infrared Waveband

All mines show negative contrast against a grass background, however, only P-4-B and SB-33, which do not show increased reflectance at the chlorophyll edge, show high contrast at all wavelengths. PFM-1 and Ranger show

moderately high contrast in this waveband. Contrast against a soil background is positive for PFM-1 and Ranger, and negative for P-4-B and SB-33 but nowhere are the contrast differences large.

At longer wavelengths in the near-infrared waveband, grass, soil, and the mines show similar reflectances with each one showing positive and negative contrasts depending upon the wavelength selected.

#### Far-infrared Measurements

The results of reflectance measurements, in the far-infrared, for two directions of polarized radiation are given for two of the mines in Figures 3 and 4. The remaining two mines yielded similar results. Data are presented over the 8  $\mu\text{m}$  to 14  $\mu\text{m}$  waveband. Differences in reflectance with polarizer angle were substantial, typically the reflectance fell to half or less of its  $0^\circ$  value on rotation of the polarizer to  $90^\circ$ . A polarization contrast between the two states exceeding 30% was shown by all of the mines.

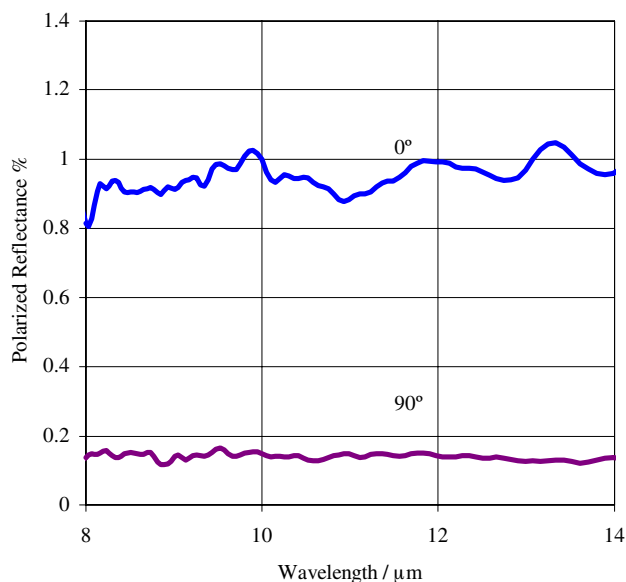


Figure 4. PFM-1 Mine Polarized Reflectance

#### Exploitation of Reflectivity Differences

Practical mine detection equipment needs to be rugged, reliable, and relatively inexpensive so that it can be widely available to the demining community. Image intensifiers with photocathodes sensitive to UV radiation, and lead sulphide array imagers for the NIR, are currently available at reasonable cost suggesting their use as detectors. Modern staring array technology is yielding better and better quality far-infrared thermal detector systems at much reduced cost,<sup>4,5</sup> thus offering the possibility of a cheap, polarization enhanced far-infrared mine detector.

### The Ultra-Violet Waveband

Image intensifier (II) techniques look most suitable for the ultra-violet waveband utilizing sunlight as illumination and the reasonably high transmission of the atmosphere over a range of about 100 m. Although solar irradiance is falling sharply across this waveband, the gain available from image intensifiers (about  $10^5$ ) compensates for lower irradiance at shorter wavelengths.

The more common window glasses used in II tubes absorb UV radiation so special thin UV-transmitting glass or fused silica windows are required. Most of the common photocathode materials are sensitive to UV radiation. UV absorption in the imaging optics may also limit the use of readily available II sights. These considerations and that of high reflectivities form flowers in the UV A, leads to an optimum band for detection of 300nm to 350 nm.

Experiments with an intensified CCD camera fitted with a narrow band filter centered at 337 nm have shown the ease with which mines can be detected as may be seen in the Figures 5 and 6 in which show the grass background and a P-4-B mine that has been sown in the twelve-inch high grass.

### The Near-infrared Waveband

Close to the chlorophyll edge, solar illumination is plentiful, so either lead sulphide array cameras or image intensifiers might be used, as modern II sights have a sensitivity which extends to about 900 nm. Such a device, if fitted with a long-wave-pass filter with a cut-on wavelength of about 800 nm or a narrow band-pass filter centred between 800nm and 900nm, should be capable of exploiting the contrast between mines and both grass and soil backgrounds. However, the variability of contrast between mines and their backgrounds would require careful interpretation for reliable detection to be made.

### The Far-infrared Waveband

Modern uncooled staring array thermal detectors when coupled to a rotating polarizing element offer a promising device for background suppression and hence enhanced mine detection. The reflection and emission polarization states are linked and, after suitable difference processing,<sup>6,7</sup> the target (mine) can be readily visualized.

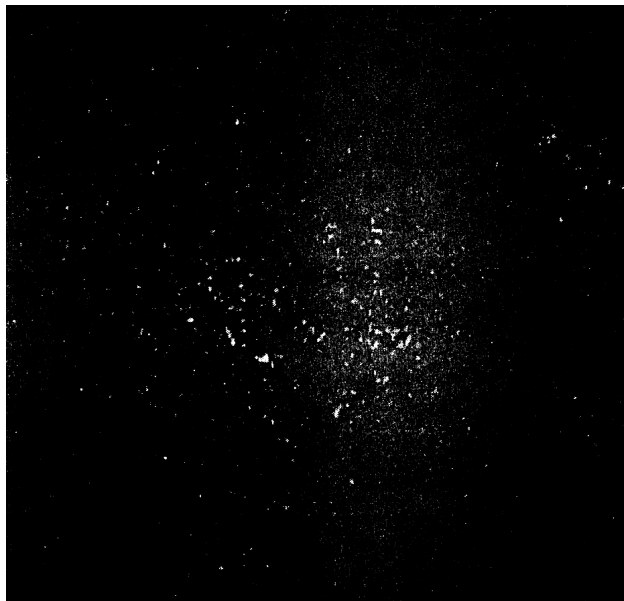


Figure 5. Ultra-violet Image of Grass Background

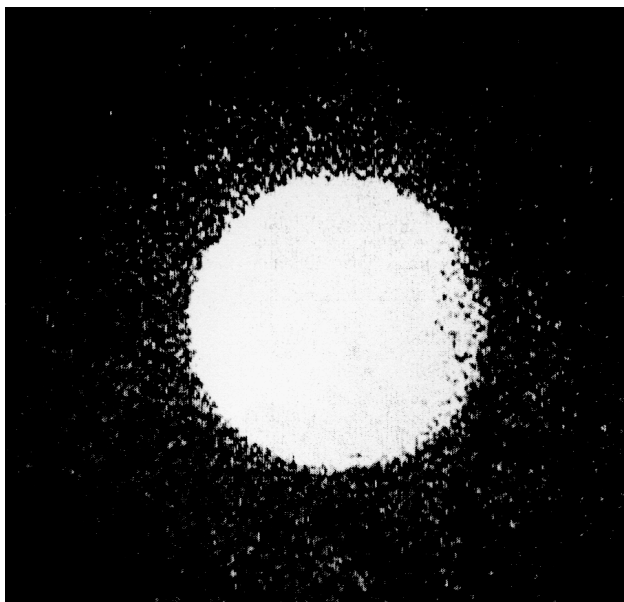


Figure 6. Ultra-violet Image of P-4-B Mine in Grass

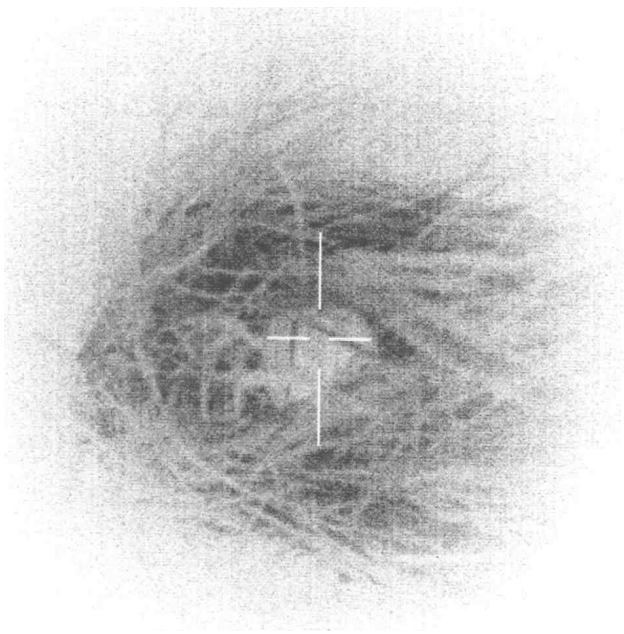


Figure 7. Polarized Infrared Image  $90^\circ$

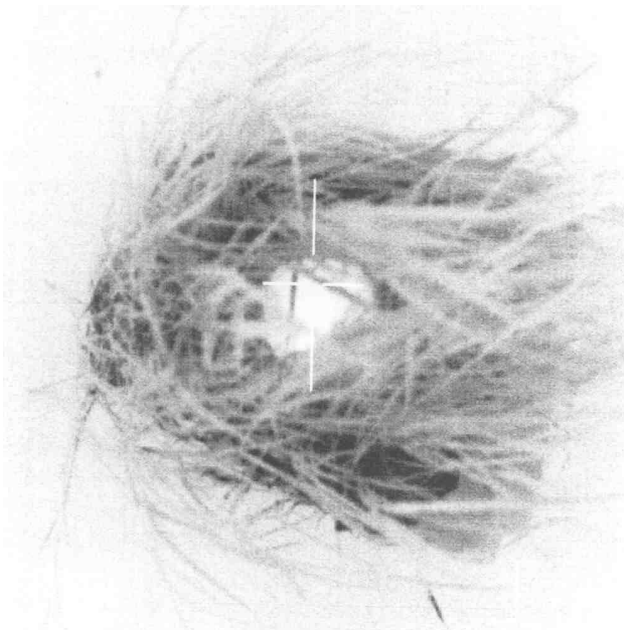


Figure 8. Polarized Infrared Image  $0^\circ$

Figures 7 and 8 show a Ranger mine sown in 12 inch high grass viewed by a thermal imager at  $30^\circ$  incidence with the polarizer set at two angles  $90^\circ$  apart. The differences in polarized reflectance measured in the laboratory are clearly seen in the thermal image, suggesting that a device with a continuously rotating polarizer would yield an image modulated at twice the polarizer rotation rate.

## Conclusions

Landmine detection comprises one part of a mine clearing operation which, depending upon the particular situation, might be assisted by electro-optic detection devices.

We have shown that scatterable anti-personnel landmines show high contrast with respect to their anticipated backgrounds across the ultra-violet waveband and to a lesser extent in the near-infrared waveband as well. The contrasts shown are typically larger than those found in other wavebands. The polarization of reflectance and emission in the far-infrared waveband can be exploited to reduce scene clutter and enhance mine detection.

The technology to exploit these wavebands is available now, and is becoming less costly to implement in practical devices.

More work needs to be done to demonstrate the general applicability of these chosen wavebands to a wider range of mines in a true minefield environment.

## References

1. ICRC Banning anti-personnel mines : the Ottawa treaty explained. Geneva 1998
2. Norbury S. Detection of scatterable land mines using ultra violet frequencies. M Sc Project Report Cranfield University 1999
3. Richardson et al. Surveillance & target acquisition systems. 2<sup>nd</sup> Edition Brassey's Land Warfare 1997.
4. Watton R et al. Uncooled infrared imaging using pyroelectric arrays. J. Defence Science 1998, 3, 150.
5. Hollins R et al. Electronics and electro-optics for the 2030 timeframe. J. Defence Science 2000, 5, 12.
6. Jordan D L and Lewis G D. Passive polarization discrimination for the reduction of clutter in thermal images. J. Defence Science 1998, 3, 183.
7. De Jong W et al. Usage of polarization features of land mines for improved automatic detection. SPIE 2000, 4038, 29.